Thermal Decomposition of Ammonium Dinitramide at Moderate and High Temperatures

Sergey Vyazovkin and Charles A. Wight*

Department of Chemistry, University of Utah, Salt Lake City, Utah 84112

Received: October 9, 1996; In Final Form: June 18, 1997[⊗]

Temperature-controlled gas cell and thin film laser pyrolysis techniques have been used to investigate the condensed phase thermal decomposition of ammonium dinitramide (ADN). Gas cell experiments have been performed at heating rates of $10^{-2}-10^{-1}$ °C s^{-1} and in a temperature region 20−250 °C. Pulsed CO_2 laser heating of thin ADN films has allowed heating rates of 10^7 °C s^{-1} and temperatures of about 630 °C to be reached. The thermal decomposition products have been monitored by FTIR spectroscopy. Both experimental techniques show that the primary decomposition products are N_2O and NO_2. Nitric oxide is produced at a later stage in the reaction. No evidence has been found for participation of dinitramidic acid in the reaction mechanism. The fact that the same initial products are observed over a wide range of temperatures and heating rates shows that this mechanism can be used to model the initial stages of combustion of ADN.

Introduction

Ammonium dinitramide (ADN) is a powerful oxidizer that is a potential halogen-free replacement for ammonium perchlorate in solid rocket propellants. A detailed knowledge of the mechanism and kinetics of ADN thermal decomposition is required to predict characteristics of its combustion. Mechanistic studies of ADN thermal decomposition were carried out by Rossi et al.[1] by mass spectrometry and Brill et al.[2] by a *T*-jump/FTIR technique.

Recently, we reported[3] a study of condensed phase thermal decomposition of ADN using differential scanning calorimetry (DSC) and thermogravimetry coupled with mass spectrometry (TG−MS). Conditions favoring condensed phase decomposition were accomplished by performing experiments at ambient pressure and moderate temperatures (i.e., slow heating rates). Our TG−MS experiments showed[3] that formation of gaseous reaction products occurs in two distinct stages. The first products detected are N_2O, NO, and NO_2. They are followed at a later stage by H_2O, HONO, NH_3, and HNO_3. Because no NH_3 was detected in the early stages of ADN decomposition, we suggested that the process follows an ionic mechanism involving formation of ammonium nitrate (AN) and ammonium mononitramide by two parallel reaction channels,

$$NH_4N(NO_2)_2 \rightarrow N_2O + NH_4NO_3 \quad (1)$$

$$NH_4N(NO_2)_2 \rightarrow NO_2 + NH_4NNO_2 \quad (2)$$

The mononitramide ion (NNO_2^-) subsequently dissociates[4] via

$$NNO_2^- \rightarrow NO^- + NO \quad (3)$$

The net reaction for steps 2 and 3 is

$$NH_4N(NO_2)_2 \rightarrow NO_2 + NO + NH_4NO \quad (4)$$

One of the potential difficulties associated with a reaction mechanism derived from slow heating data is that it may not be applicable to realistic combustion conditions. That is, the high heating rates and temperatures associated with propellant combustion may favor other reaction channels that are not detected in slow heating experiments. There is some evidence that the surface temperature of burning ADN is approximately 300 °C.[2] For this reason, we initiated the present study in which the condensed phase thermal decomposition of ADN has been investigated over a wide temperature interval. The main purpose of the work is to determine if the reaction mechanism changes when passing from moderate temperatures and slow heating rates to high temperatures and fast heating rates. At moderate temperatures (less than 250 °C), the thermal decomposition of ADN has been studied by heating in an infrared gas cell. High temperatures of decomposition (about 630 °C) have been reached by pulsed laser heating of thin films of ADN. In both cases, decomposition products have been monitored by transmission FTIR spectroscopy.

Experimental Section

A 1 g sample of crystalline ADN was kindly supplied by Thiokol Corp. It was stored at room temperature in the dark (to avoid photochemical degradation) and was used in our experiments as supplied with no further purification. The melting point of this material, reported earlier,[3] indicates that it may have as much as 3% impurity of ammonium nitrate, a primary thermal decomposition product. The temperature-controlled infrared gas cell (Wilmad Glass) is a stainless steel tube with two gas ports equipped with needle valves. To avoid possible heterogeneous reactions on the steel surface, the interior of the gas cell was coated with Teflon. Both ends of the cell are covered with NaCl windows. The cell temperature is programmed using an Omega CN76000 temperature controller unit that senses the cell temperature by means of an iron−constantan (type J) thermocouple and delivers power to the cell through a 275 W heater coil. Samples of ADN (2−3 mg) were placed in the gas cell and flushed with dry nitrogen for 10 min before initiating a linear heating program. Similarly, we have performed two reference heated cell experiments with ammonium nitrate (Mallinckrodt, 99.8% purity).

A Mattson Research Series FTIR spectrometer was used to monitor reaction products. Spectra were collected in the kinetic mode by averaging 8−16 scans at 1−2 cm^{-1} resolution. As many as 250 spectra were collected during each experiment.

The experimental procedure for the thin film laser pyrolysis has been described elsewhere,[5] and only a brief outline is presented here. Each thin film sample of ADN was deposited

* To whom correspondence should be addressed. Email: wight@chemistry.utah.edu.

⊗ Abstract published in *Advance ACS Abstracts,* August 15, 1997.

S1089-5639(96)03116-7 CCC: $14.00

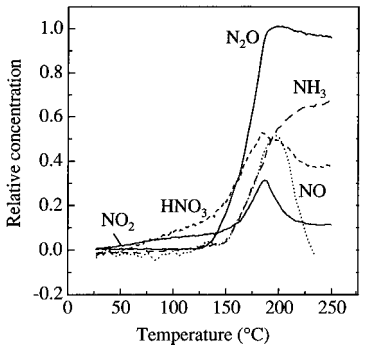

Figure 1. Relative concentrations for gaseous reaction products of ADN decomposition during heating in a Teflon-coated static gas cell at 5 °C min^{-1}.

onto a 25 mm diameter CsI window from a dilute methanol solution (1 mg of ADN per 1 mL of methanol) using an airbrush. The film, which is typically 0.75 μm thick in this study, was thoroughly dried to remove the methanol solvent. A second CsI window was then placed over the sample, and the "sandwich" arrangement was mounted in a vacuum Dewar cell and cooled to 77 K. The sample was then irradiated by pulses from a CO_2 laser (Pulse Systems LP140-G) tuned to the P(34) line at 1033 cm^{-1}. The laser has a nominal pulse length of 35 μs and was used at a repetition rate of 1 Hz. Fluence of the laser pulses was varied over the range 0.2−2 J cm^{-2} by means of a concave focusing mirror. This technique allows one to heat the sample from 77 K to approximately 900 K (630 °C) during the laser pulse. The thin film, being in contact with a relatively massive substrate at 77 K, is cooled with a characteristic time estimated to be 30 μs to 1 ms, depending on the film thickness.[5] IR spectra were obtained before and after laser pyrolysis to record any physical or chemical changes in the sample. Spectra were collected by averaging 32 scans at 0.25 cm^{-1} resolution.

Results

Thermal Decomposition of ADN in Gas Cell. In the gas cell experiments, the temperature was scanned from 20 to 250 °C with linear heating rates of 1.5−20 °C min^{-1}. Major detected gaseous products of ADN decomposition were N_2O, NO_2, NO, NH_3, and HNO_3. The gases were monitored by their respective absorption bands at 2224,[6] 1621,[6] 1903,[6] 966,[7] and 1709 cm^{-1}.[8] The absorption intensities of these bands have been converted to the relative concentrations using scaling factors reported by Brill et al.[9] The resulting kinetic curves are shown in Figure 1.

Because of the high sensitivity of FTIR technique, the first decomposition product (NO_2) was detected at about 50 °C. This temperature is approximately 80 °C lower than the initial temperature of the thermal decomposition detected in TG−MS and DSC experiments.[3] Evolution of NO_2 is almost immediately followed by formation of HNO_3 . Most of the N_2O is formed at a somewhat later stage; however, it is detectable at temperatures as low as 50 °C because of the high detection sensitivity for this molecule. In contrast, the formation of NO and NH_3 is observed only above 100 °C.

Reference experiments on the thermal decomposition of ammonium nitrate have shown that the primary products of decomposition are HNO_3 and NH_3, which appear in equal amounts over the range 60−120 °C. Additional products (NO, NO_2, and N_2O) become observable only at about 150 °C.

Laser Pyrolysis of ADN Thin Films. The first series of experiments was performed on a single sample, which was irradiated with single pulses at successively increasing laser

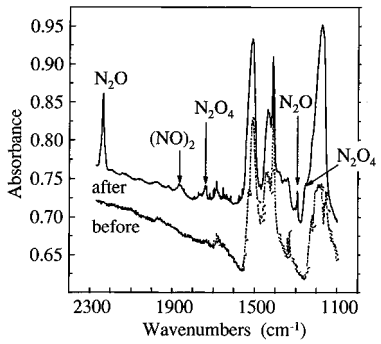

Figure 2. Spectra of a thin film of ADN at 77 K before (dotted line) and after (solid line) laser pyrolysis at 2.07 J cm^{-2}.

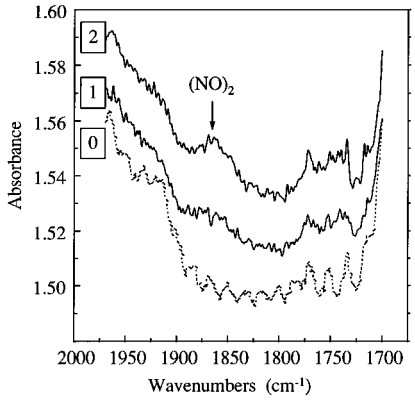

Figure 3. Formation of nitric oxide dimer in a series of successive laser pyrolysis periods (five laser pulses each at 1.0 J cm^{-2}): (0) ADN spectrum before pyrolysis; (1) after 7th pyrolysis period; (2) after 14th pyrolysis period.

TABLE 1: Assignment of the Absorption Bands in FTIR Spectrum of Pyrolyzed ADN

observed band/cm^{-1}	assignt	ref band/cm^{-1}
3507	N_2O	3500[10]
2579	N_2O	2580[10]
2236	N_2O	2244[10]
1864	$(NO)_2$	1862−1866;[13] 1865[15]
1739	N_2O_4	1739;[5] 1734, 1760;[11] 1728, 1749;[12] 1730[14]
1293	N_2O	1295[10]
1255	N_2O_4	1256;[11] 1255;[12] 1253[14]
589	N_2O	595[10]

fluences: 0.94, 1.50, 1.98, and 2.07 J cm^{-2}. Figure 2 shows the most informative part of the infrared spectrum of ADN pyrolyzed at 2.07 J cm^{-2}. A complete list of new absorption bands that appeared in the spectrum of pyrolyzed ADN is given in Table 1. The bands have been identified as the following products of decomposition: N_2O,[10] N_2O_4 (dimer of NO_2),[5,11−14] and $(NO)_2$ (dimer of NO).[13,15] It is noteworthy that N_2O and N_2O_4 were detected after the first pyrolysis at 0.94 J cm^{-2}, whereas $(NO)_2$ was detected only after pyrolysis at 2.07 J cm^{-2}.

A second series of experiments was carried out by subjecting a single sample to 14 successive pyrolyses of 5 pulses each at 1.0 J cm^{-2}. In this series, N_2O and N_2O_4 were detected after the first pyrolysis, but $(NO)_2$ was observed only after the seventh pyrolysis, as shown in Figure 3.

The third series of experiments was conducted by subjecting a single sample to successively higher laser fluence starting at 0.18 J cm^{-2}. The fluence was increased gradually in order to determine the thresholds for formation of N_2O and N_2O_4. The results of these experiments are collected in Table 2. No products were observed at fluences below 0.78 J cm^{-2}. However, N_2O and N_2O_4 appeared simultaneously when the

TABLE 2: Products of Low-Fluence Laser Pyrolysis of ADN

	integrated absorbance/cm^{-1}	
fluence/J cm^{-2}	N_2O	N_2O_4
0.18		
0.28		
0.43		
0.48		
0.58		
0.70		
0.78	0.05	0.06
0.90	0.20	0.11
1.0	0.33	0.14
1.13	0.35	0.16
1.22	0.34	0.17
1.43	0.39	0.48
1.5	0.42	0.58

TABLE 3: Parameters Used in the Simulation of Thin Film Laser Pyrolysis Experiments

physical property	layer 1 ADN	layer 2 CsI	layer 3 CsI
total thickness (10^{-6} m)	0.75	22.5	0.075
number of slices	10	300	1
thermal conductivity (W m^{-1} K^{-1})	0.56[a]	1.1[b]	1.1[b]
heat capacity (10^6 J m^{-3} K^{-1})	3[c]	0.92[d]	∞[e]
IR absorptivity (10^6 m^{-1})	0.53[f]	0	0

[a] Based on the estimated heat capacity and a recent measurement of the thermal diffusivity of ammonium dinitramide (ref 22). [b] Reference 20. [c] Estimate based on the heat capacity of ammonium nitrate (ref 21). [d] Reference 21. [e] This value is required to mimic the heat-sinking properties of the apparatus. [f] Measured at 1033 cm^{-1} (this work).

sample was pyrolyzed at this fluence. This suggests that the reaction rates for the steps that produce them are essentially the same under these experimental conditions.

Although the infrared spectrum of condensed phase ammonia is well-known,[16,17] no evidence for formation of NH_3 was observed in spectra of ADN films subjected to laser pyrolysis.

Modeling of Laser Pyrolysis Experiments

To carry out laser pyrolysis of a thin film, it must have a significant absorption cross section at the frequency of the laser. Otherwise, the sample must be heated indirectly by means of a second layer that absorbs the radiation and transfers the heat to the layer of interest by conduction.[18] ADN has an infrared absorptivity of about 5.3×10^5 m^{-1} at 1033 cm^{-1}, which corresponds to the P(34) line of the CO_2 laser 001−020 transition. This means that a 0.75 μm film will absorb 33% of the laser pulse energy.

The films are too thin and the heating too fast to measure temperature profiles using transducers embedded in the films. To get a rough idea of the time and temperature scales involved in this type of experiment, we wrote a computer program to simulate the heating and cooling process. The parameters used in the calculation are the best available room temperature values and are listed in Table 3. The calculation was performed by dividing the sample into 0.075 μm slices (10 slices of ADN and 300 of the underlying CsI supporting window, plus one slice at 77 K that has the thermal conductivity of CsI but infinite heat capacity). This geometry is indicated schematically in Figure 4. During the first 35 μs of the simulation, each slice of ADN absorbed energy from the laser appropriate to its thickness and absorption coefficient. The laser beam intensity was assumed to be spatially and temporally uniform. Each time step of the simulation (1.6 ns) involved solving the one-dimensional heat diffusion equation using the Crank−Nicholson algorithm,[19] which is accurate to second-order in both space and time, to estimate the rate at which the heat is conducted from the ADN into the relatively massive CsI window. Although the actual samples employed a "sandwich" configuration that includes a CsI cover window, the simulations were conducted assuming that the sample is cooled from one side only because the thermal contact between the sample and cover window was poor. The results of the simulation are illustrated in Figure 4. The rate of heat transfer into the support window is very fast, and the temperature profile across the thin ADN film is fairly uniform. This is because the thermal diffusivity of cesium iodide (1.2×10^{-6} m^2/s)[20,21] is much higher than that of ADN (1.87×10^{-7} m^2/s).[22] The calculated peak temperature for a 2.07 J cm^{-2} irradiation is about 1100 K (827 °C). However, melting of the CsI surface (which was not included in the simulation) limits the temperature of the sample to about 630 °C.

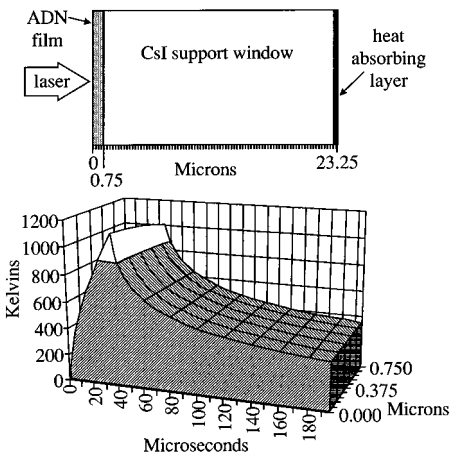

Figure 4. Calculated temperature distribution during laser pyrolysis of a 0.75 μm film of ADN on a massive CsI window. The laser pulse duration is 35 μs at a total fluence of 2.07 J cm^{-2}. The initial temperature of the film is 77 K. The thermal parameters used in the calculation are given in Table 3. Peak temperatures are probably limited to about 900 K by transient melting of the CsI surface (see text).

Although this calculation is useful for illustrating some of the gross features of the thin film laser pyrolysis experiment, the results should not be regarded as being quantitatively accurate. This is because the simulation is based on an estimated heat capacity for ADN, and no attempt was made to account for the temperature dependence of the heat capacity or thermal conductivity of either ADN or CsI. No attempt was made to account for reduced thermal conductivity at the interface between the two materials, for transient melting of the CsI, or for details of the laser pulse shape (temporal or spatial).

Given the limitations of the calculation, it nevertheless provides a qualitatively useful estimate of the heating rate (2×10^7 °C s^{-1}), peak temperature (630 °C), and duration of the heating event (30 μs) for the experimental conditions employed in our study.

Discussion

Thermal Decomposition of ADN in Gas Cell. Unlike the TG−MS experiments,[3] which were performed in a flowing atmosphere of argon, the current gas cell experiments were carried out in a static atmosphere (initially, N_2). While the temperature rises, evolved gases from the decomposition of ADN are allowed to accumulate in the gas cell. Obviously, this provides an opportunity for gas-phase reactions to occur between accumulated gaseous products or between the gases and condensed phase species. The effects of such reactions will be most prominent near the end of the experiment. Indeed,

Figure 1 shows that the relative concentrations for N_2O, NO_2, HNO_3, and NO decrease at temperatures above 200 °C (i.e., after all the ADN has been gasified and only gas-phase reactions are possible).

A set of heated gas cell experiments were initially performed in this apparatus with uncoated stainless steel walls. Under these conditions, reductions in the amounts of NO_2 and NH_3 were more pronounced in the latter stages of the heating program. The Teflon coating reduced the effects of heterogeneous reactions of these two products. The first products observed (at low temperatures) are representative of the condensed phase decomposition of ADN; the results in this region are qualitatively similar in both sets of experiments (coated and uncoated cells).

The only major gas-phase product not shown in Figure 1 is water vapor. A control experiment run with no ADN sample showed that most of the water results from outgassing from the cell walls. However, our earlier TG−MS study[3] showed that some water is produced by the decomposition reaction as well.

The first conclusion that can be drawn from the gas cell experiments (Figure 1) is that the primary decomposition products are NO_2 and N_2O. The nitric acid observed in the gas cell experiments is most likely a secondary product of the reaction of $NO_2 + H_2O$, the latter of which is produced by outgassing of the cell walls. The observation of NO_2 and N_2O as initial products is completely consistent with the mechanism that we proposed earlier[3] on the basis of TG−MS data. In similar gas cell experiments, Russell et al.[23,24] detected the formation of N_2O at low temperature (60 °C). However, NO_2 was observed in their experiments only at temperatures higher than 130 °C. Their proposed mechanism[23,24] is similar to ours in that two channels are operative, the first being intramolecular O atom transfer forming N_2O and ammonium nitrate. However, the second (higher temperature) channel in their mechanism starts with proton transfer forming ammonia and dinitramidic acid,

$$NH_4N(NO_2)_2 \rightarrow NH_3 + HN(NO_2)_2 \qquad (5)$$

followed by N−N bond scission, liberating NO_2:

$$HN(NO_2)_2 \rightarrow HNNO_2 + NO_2 \qquad (6)$$

The principal reason why we favor N−N bond scission and formation of ammonium mononitramide salt (reaction 4) rather than the acid (reaction 5) is that the NH_3 observed in our experiments (both infrared and TG−MS) appears well after formation of NO_2. In the TG−MS experiments, this point was somewhat ambiguous because fragmentation of NO_2 in the electron-impact ionizer gives rise to an NO^+ daughter ion at $m/z = 30$, making it difficult to completely separate the NO_2 and NO product channels. However, the infrared gas cell experiments provide clear and unambiguous evidence that NO_2 is produced at temperatures at least 50 °C below the point where NO and NH_3 are observed. Therefore, reaction 5 is not the primary step of the condensed phase decomposition of ADN as was postulated in other mechanisms.[1,2,23,24]

It is interesting to note that the kinetic curves of the formation of NO_2 and N_2O (Figure 1) show no obvious singularity at the melting point of ADN (92 °C). This means that the mechanism of the thermal decomposition of ADN almost certainly remains the same when changing from the bulk solid to the bulk liquid phase. However, if reaction occurs exclusively at the surface, then a liquid mixture of ADN and AN can exist at temperatures as low as 55 °C.[23,24]

We carried out control experiments in which AN was decomposed by slow heating in the IR gas cell in order to determine which ADN products might be formed as a result of AN decomposition. Although previous studies have shown[25] that pure solid AN starts to markedly decompose only above 170 °C, which is the melting point, our reference experiments on AN decomposition revealed that equal amounts of NH_3 and HNO_3 are simultaneously formed from AN in the range 60−120 °C, whereas NO, NO_2, and N_2O become detectable at 150 °C (close to the melting point of AN). Nitric acid was observed in the ADN decomposition experiments, but it appears at much lower temperatures than NH_3. This observation is good evidence that HNO_3 is formed by a different mechanism in this case, most likely by reaction with water vapor in the heated cell. We cannot completely exclude the possibility that AN formed during ADN decomposition may exist in the liquid state at temperatures below the melting point because of formation of an eutectic with ADN.[23,24] However, if decomposed, AN would give rise to equal amounts of NH_3 and HNO_3 in the earlier stages of the reaction, which is contrary to our observations.[25,26]

Laser Pyrolysis of ADN Thin Film. Whereas TG−MS and gas cell experiments have been performed at moderate temperatures (below 250 °C) and rather slow heating rates (1−20 °C min^{-1}), laser heating allows the conditions more characteristic of combustion (high temperatures and rapid heating) to be reached. With increasing temperature, the relative contribution of the reaction pathways to the overall process changes in accord with the activation energies of the pathways. As the result, we generally cannot expect the distribution of the reaction products to remain unchanged for decomposition carried out in different temperature regions. Interestingly, our TG studies (temperature interval 130−250 °C) of the overall kinetics of ADN thermal decomposition (i.e., conversion to gaseous products) showed[3] that the effective activation energy of the process varies with conversion in the interval 125−175 kJ mol^{-1}. Because the first step of reaction involves formation of gaseous products, this indicated to us that the two parallel pathways leading to formation of NO_2 and N_2O have rather different activation energies. According to the gas cell experiments, reaction 1 starts somewhat later than reaction 2, which allows us to assume that this pathway has a higher activation energy. If this is really the case, then the conditions of laser heating should favor the pathway leading to formation of N_2O. In any case, we felt that the laser pyrolysis experiments were an essential test to verify the potential applicability of the "moderate temperature mechanism", reactions 1−4, to conditions realized during combustion of ADN.

The results of the laser pyrolysis experiments seem to be quite consistent with "the moderate temperature mechanism". First, the fact that at higher temperatures N_2O forms simultaneously with NO_2 (detectable as N_2O_4; see Table 2) agrees well with the occurrence of the two competing channels with reaction 1 having a higher activation energy. Second, the fact that NO (detectable as $(NO)_2$) forms markedly later than both NO_2 and N_2O is fully in accord with pathway 3, in which NO is formed as a product of secondary reactions.

In principle, the NO_2 formed in the laser pyrolysis experiments could arise from secondary decomposition of AN formed in reaction 1. At high temperatures (above 290 °C), AN decomposes by a radical mechanism,[26] giving rise to formation of N_2O, NO_2, NO, HNO_3, and NH_3 at rapid heating.[2] However, if formation of NO_2 were only due to AN decomposition, then NH_3 should have been detected among the products of the laser pyrolysis of ADN. The fact that formation of both NO_2 and

NO was observed without detecting NH_3 in the laser pyrolysis experiments is evidence that these products arise from decomposition of ADN via reaction 2. The absence of NH_3 among the laser pyrolysis products is likely due to low extents of ADN conversion reached in the experiments (i.e., the ammonia remains tied up as ammonium salts until later stages of the overall reaction). Overall, the results of the laser pyrolysis experiments provide evidence that a single mechanism can account for decomposition of ADN over a wide range of temperatures and heating rates.

Conclusions

The thermal decomposition of ADN has been studied using a temperature-controlled gas cell at temperatures below 250 °C and by thin film laser pyrolysis at temperatures as high as about 630 °C. Despite the significant difference in the temperature regions, both techniques have shown that the primary products of the condensed phase decomposition of ADN are N_2O and NO_2, which are followed by NO at a later stage. These results are in complete agreement with a reaction mechanism proposed earlier on the basis of TG−MS experiments. The current study suggests that this mechanism can be used to model the decomposition of ADN even under the extreme conditions appropriate to combustion of solid rocket propellants.

Acknowledgment. This research is supported by the Office of Naval Research and Program Officer Dr. Richard S. Miller under Contract No. N00014-95-1339. We are grateful to Dr. Robert Wardle of Thiokol Corporation for providing the sample of ADN.

References and Notes

(1) Rossi, M. J.; Bottaro, J. C.; McMillen, D. F. *Int. J. Chem. Kinet.* **1993**, *25*, 549.

(2) Brill, T. B.; Brush, P. J.; Patil, D. G. *Combust. Flame* **1993**, *92*, 178.

(3) Vyazovkin, S.; Wight, C. A. *J. Phys. Chem. A* **1997**, *101*, 5653.

(4) Barlow, S. E.; Bierbaum, V. M. *J. Phys. Chem.* **1990**, *92*, 3442.

(5) Botcher, T. R.; Wight, C. A. *J. Phys. Chem.* **1994**, *98*, 5441.

(6) Huber, K. P.; Herzberg, G. *Constants of Diatomic Molecules*; Van Nostrand Reinhold: New York, 1979.

(7) Burgess, J. S. *Phys. Rev.* **1949**, *76*, 1267.

(8) Cohn, H.; Ingold, C. K.; Poole, H. G. *J. Chem. Soc.* **1952**, 4272.

(9) Brill, T. B.; Arisawa, H.; Brush, P. J.; Gongwer, P. E.; Williams, G. K. *J. Chem. Phys.* **1995**, *99*, 1384.

(10) Giguere, P. A.; Harvey, K. B. *Spectrochim. Acta* **1957**, *9*, 204.

(11) Wiener, R. N.; Nixon, E. R. *J. Chem. Phys.* **1957**, *26*, 906.

(12) Snyder, R. G.; Hisatsune, I. C. *J. Chem. Phys.* **1957**, *26*, 960.

(13) Fateley, W. G.; Bent, H. A.; Crawford, B. *J. Chem. Phys.* **1959**, *31*, 204.

(14) Hisatsune, I. C.; Devlin, J. P.; Wada, Y. *J. Chem. Phys.* **1960**, *33*, 714.

(15) Smith, A. L.; Keller, W. E.; Johnston, H. L. *J. Chem. Phys.* **1951**, *19*, 189.

(16) Reding, F. P.; Hornig, D. F. *J. Chem. Phys.* **1951**, *19*, 594.

(17) Staats, P. A.; Morgan, H. W. , *J. Chem. Phys.* **1959**, *31*, 553.

(18) Botcher, T. R.; Beardall, D. J.; Wight, C. A.; Fan, L.; Burkey, T. J. *J. Phys. Chem.* **1996**, *100*, 8802.

(19) Press, W. H.; Flannery, B. P.; Teukolsky, S. A.; Vetterling, W. T. *Numerical Recipes in C*; Cambridge University Press: Cambridge, 1988; p 659.

(20) Powell, R. L.; Childs, G. E. In *American Instititute Physics Handbook*, 3rd ed.; Gray, D. E., Ed.; McGraw-Hill: New York, 1972.

(21) *CRC Handbook of Chemistry and Physics*, 74th ed.; Lide, D. R., Ed.; CRC Press: Boca Raton, FL, 1993.

(22) Hansen-Parr, D. Unpublished results.

(23) Russell, T. P.; Stern, A. G.; Koppes, W. M.; Bedford, D. C. In Proceedings of JANNAF Combustion Meeting, Hampton, VA, October 19−23, 1992; CPIA Publication, 1992.

(24) Russell, T. P.; Piermarini, G. J.; Block, S.; Miller, P. J. *J. Phys. Chem.* **1996**, *100*, 3248.

(25) Rosser, W. A.; Inami, S. H.; Wise, H. *J. Phys. Chem.* **1963**, *67*, 1753.

(26) Brower, K. R.; Oxley, J. C.; Tewari, M. *J. Phys. Chem.* **1989**, *93*, 4029.